ELSEVIER

Ceramics International 31 (2005) 1097–1101

CERAMICS INTERNATIONAL

www.elsevier.com/locate/ceramint

Effect of various dopants on the tunable and dielectric properties of $Ba_{0.6}Sr_{0.4}TiO_3$ ceramics

Rui-Hong Liang *, Xian-Lin Dong, Ying Chen, Fei Cao, Yong-Ling Wang

Shanghai Institute of Ceramics, Chinese Academy of Sciences, 1295 Dingxi Road, Shanghai 200050, PR China

Received 6 June 2004; received in revised form 29 October 2004; accepted 2 December 2004
Available online 5 February 2005

Abstract

Acceptor (Mn-, Co-) doped and donor Y-doped $Ba_{0.6}Sr_{0.4}TiO_3$ have been prepared by traditional ceramic processing and their structural, surface morphological, dielectric and tunable properties were investigated. The results show all dopants to have a strong effect on the average grain size. The curie temperature of all doped specimens decreases and their temperature spectrum broadens. Loss tangent at 15 °C and low frequency (10 kHz) increases for all doped specimens whereas the loss tangent at high frequency (100 MHz) is not affected. The tunability of all the doped specimens is lower than the undoped one.

Keywords: C. Dielectric properties; D. $BaTiO_3$ and titanates; Tunable properties; Functional application

1. Introduction

Present phased-array antennas are constructed using ferrite phase shifting elements. These elements are ferromagnetic and current driven, where the phase shift is caused by a change in the permeability of the material. The performance of these type phase shifter is good, however, they are very costly, large, and heavy. In order to make these devices more practical and smaller, better materials must be developed. Recently there has been growing interest in the use of barium strontium titanate (BST) for high performance microwave tunable devices, such as phase shifters, tunable filters, steerable antennas, because of the strong dependence of the dielectric properties on the electric field [1–3]. The use of ferroelectric BST as phase shifting elements can reduce the volume, cost and weight of the phase shifter greatly. For this use, a BST system is expected to possess the following characteristics: low dielectric constant (ε_r), large tunability ($(\varepsilon_{r(0)} - \varepsilon_{r(app)})/\varepsilon_{r(0)}$), low loss tangent ($\tan\delta$) and good thermal stability. The tunability of specimens affects the specimens' properties through the changes of the dielectric constant with applied electric field. Higher tunability is desirable. The reduction of the dielectric constant reduces the overall impedance mismatch. The low loss tangent serves to decrease the insertion loss. In general, the loss tangent of BST at paraelectric phase is lower than ferroelectric phase, so BST system at paraelectric phase is desirable. There are two biggest obstacles to be overcome: one is how to reduce the loss tangent at microwave frequency; the other is how to promise comparatively high tunability when reducing its dielectric constant. So, it is very important to study the dc field effect of the dielectric behavior of BST system at paraelectric phase.

It is widely known that the dielectric properties of BST can be modified through partial substitution of isovalent or heterovalent cations at Ti sites (B-site doping) and Ba sites (A-site doping). For example, generally the acceptor (Mn, Fe) doped BST can decrease the loss tangent [4]. However, there are few paper on the dielectric constant as a function of dc field dependence. In this paper, we study the dielectric and tunable properties of the acceptor and donor doping $Ba_{0.6}Sr_{0.4}TiO_3$. The dielectric and tunable properties of $Ba_{0.6}Sr_{0.4}Ti_{0.99}M_{0.01}O_3$ (M = Mn, Co) and $(Ba_{0.6}Sr_{0.4})_{0.99}Y_{0.01}TiO_3$ have been measured under a dc-biasing field in an effort to obtain more experimental data to

* Corresponding author. Tel.: +86 21 5241 2005; fax: +86 21 5241 3903.
E-mail address: rainbow@mail.sic.ac.cn (R.-H. Liang).

0272-8842/$30.00
doi:10.1016/j.ceramint.2004.12.002

Table 1
The purity and main impurities in the starting material

The starting material	Purity (%)	Main impurity
$BaCO_3$	≥99.00	OH^- (≤0.2%), Sr^{2+} (≤0.1%), SO_4^{2-} (≤0.05%), Ca^{2+}≤ (≤0.01%)
$SrCO_3$	≥99.00	Ca^{2+} (≤0.05%), Ba^{2+} (≤0.05%), SO_4^{2-} (≤0.01%)
TiO_2	≥98.56	SiO_2 (≤0.14%), Ca^{2+} (≤0.11%)
Co_2O_3	≥98.50	Alkali metals (≤1.0%), Ni^+ (≤0.50%), Cu^{2+} (≤0.10%) SO_4^{2-} (≤0.10%)
$MnCO_3$	≥98.00	Alkali metals (≤1.5%), nitride (≤0.10%)
Y_2O_3	≥99.00	Tm_2O_3 (≤0.10%)

understand the effects of the dc electrical field on the dielectric behavior of the BST system.

2. Experimental procedure

2.1. Samples preparation

The acceptor doping $Ba_{0.6}Sr_{0.4}M_{0.01}Ti_{0.99}O_3$, where M = Mn, Co, and donor doping $(Ba_{0.6}Sr_{0.4})_{0.99}Y_{0.01}TiO_3$ were prepared by traditional ceramic processing. The starting materials are $BaCO_3$, $SrCO_3$, TiO_2, Co_2O_3, Y_2O_3, and $MnCO_3$. The purity and main impurities in the starting material are listed in Table 1. The materials were weighed according to the stoichiometric proportions, milled with alcohol and agate balls for 24 h. The dried powders were then calcined in air at 1150 °C for 2 h on recrystallised alumina crucibles. The calcined powders were again wet ground for 48 h. The dry calcined powders were mixed with polyvinyl alcohol (7 wt.%). The powders were then pressed into pellets 13 mm in diameter and approximately 2 mm in thickness and sintered at 1350 °C for 2 h. After sintering, the disc samples were electroded with silver paint for electrical measurements.

2.2. Characterization

The phase of these specimens was examined by X-ray diffraction with Cu Kα radiation (Rigaku RAX-10, Japan). Scanning electron microscopy (SEM, JSM-6700F, JEOL, Japan) was used to observe the surface. The dielectric constant of each sample was calculated from the measured capacitance and the specimen geometry. The capacitance was measured with an inductance–capacitance–resistance (LCR) meter (Agilent 4294A). For the tunable properties, a 1000 V dc power supply was connected to the LCR meter (PH2817) as the external dc bias electric field up to 1400 V/mm.

3. Results and discussion

Fig. 1 shows XRD patterns of the acceptor doping $Ba_{0.6}Sr_{0.4}M_{0.01}Ti_{0.99}O_3$(M = Mn, Co) and donor doping $(Ba_{0.6}Sr_{0.4})_{0.99}Y_{0.01}TiO_3$. All the doping samples show the typical XRD patterns of the perovskite structure and there is no second phase.

Fig. 2 shows the surface SEM micrographs of acceptor doping $Ba_{0.6}Sr_{0.4}M_{0.01}Ti_{0.99}O_3$ (M = Mn, Co) and donor doping $(Ba_{0.6}Sr_{0.4})_{0.99}Y_{0.01}TiO_3$. It indicates that all the dopants have a strong effect on the grain size. The sintered densities and grain sizes of all specimens are shown in Table 2. The grain size decreases greatly when adding these dopants. So these dopants (Co_2O_3, $MnCO_3$, Y_2O_3) can all be seen as an inhibitor of grain growth.

Fig. 3 shows the variation in the relative dielectric constant and the loss tangent of the acceptor doping $Ba_{0.6}Sr_{0.4}M_{0.01}Ti_{0.99}O_3$ (M = Mn, Co) and donor doping $(Ba_{0.6}Sr_{0.4})_{0.99}Y_{0.01}TiO_3$ as a function of temperature at 10 kHz. Table 3 shows the summary of measurements of different compositions at 15 °C. The figure indicates the curie temperature of the BST specimens decreases when adding these dopants. For the acceptor doping, this phenomenon is due to the occupation of Ti sites by these ions (Mn^{2+}, Co^{3+}). The substitution might produce oxygen vacancies, which lead to a 'break' of the cooperative vibration of Ti–O chains and bring about a decrease in the c/a ratio. This 'break' is responsible for the lower T_c of the doped BST [5]. The temperature spectrum broadens all the doped $Ba_{0.6}Sr_{0.4}TiO_3$, especially the Y- doped. This may be attributed to the enhancement in the degree of disorder having two ions occupying the same lattice site [6]. At temperature 15 °C, the loss tangent of all the doped samples

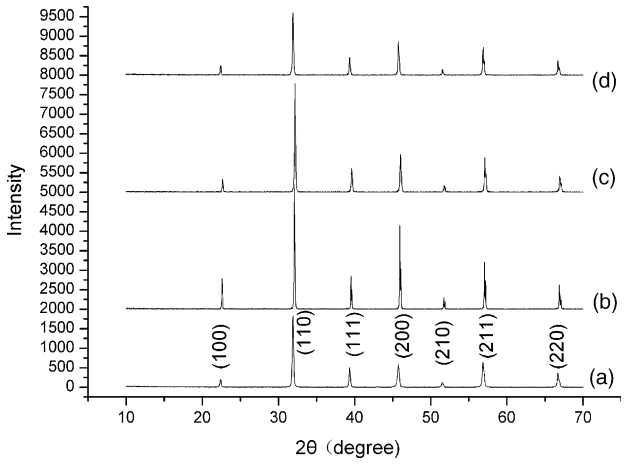

Fig. 1. XRD patterns for the doping $Ba_{0.6}Sr_{0.4}TiO_3$: (a) $Ba_{0.6}Sr_{0.4}TiO_3$; (b) $Ba_{0.6}Sr_{0.4}Mn_{0.01}Ti_{0.99}O_3$; (c) $(Ba_{0.6}Sr_{0.4})_{0.99}Y_{0.01}TiO_3$; (d) $Ba_{0.6}Sr_{0.4}Co_{0.01}Ti_{0.99}O_3$.

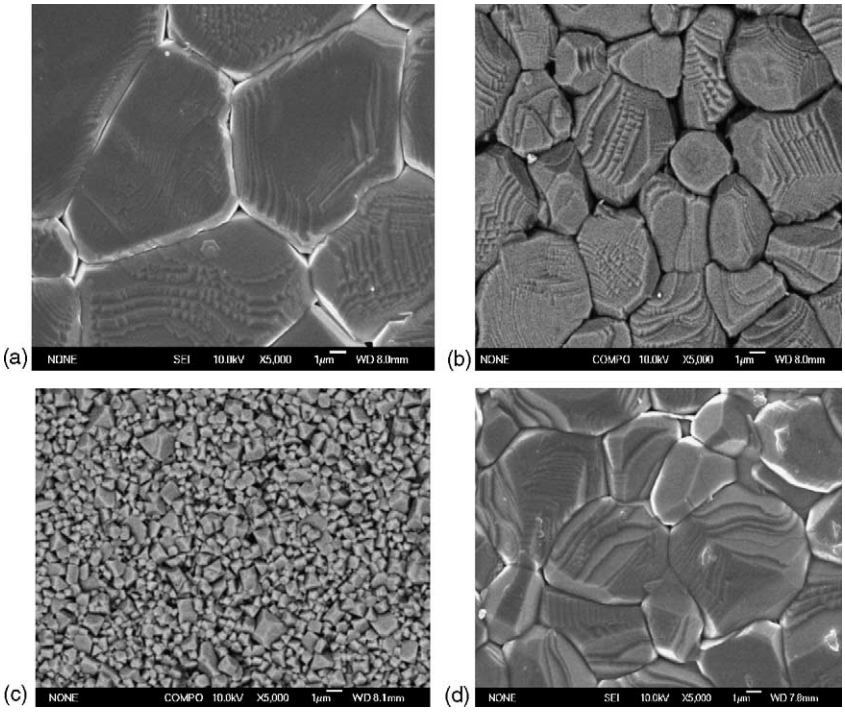

Fig. 2. SEM micrograph of the doping $Ba_{0.6}Sr_{0.4}TiO_3$: (a) $Ba_{0.6}Sr_{0.4}TiO_3$; (b) $Ba_{0.6}Sr_{0.4}Mn_{0.01}Ti_{0.99}O_3$; (c) $(Ba_{0.6}Sr_{0.4})_{0.99}Y_{0.01}TiO_3$; (d) $Ba_{0.6}Sr_{0.4}Co_{0.01}Ti_{0.99}O_3$.

increases compared with that of the undoped $Ba_{0.6}Sr_{0.4}TiO_3$ when measured at low frequency (10 kHz), especially the Y doped samples, which is shown in Table 3. This may be attributed to the Y-occupation of Ba/Sr site which probably increases the conductivity of the specimen. Because the donor impurity center bears an effective positive charge relative to the ideal lattice of the host oxide, and requires charge compensation by a species having an effective negative charge, e.g., a cation vacancy or an electron, so this increases the free carriers of the specimen and increases the loss tangent [7]. Table 3 also shows the loss tangent at high frequency (100 MHz). From the table, we can see the loss tangent of these specimens increases much compared to that at low frequency and this is probably attributed to the dielectric relaxation and phonon interaction with defect in these specimens. The loss tangent data at 100 MHz between the doped and the undoped does not vary much and the loss tangent of the doped decreases slightly than the undoped. The mechanism of the loss tangent at high frequency is not very clear and need further study. The loss tangent is still high for the tunable device application, so many researchers have added nonferroelectric oxide in it such as MgO to reduce the dielectric constant and the loss tangent at high frequency [8]. At 10 kHz, the about one degree error in the T_c and the 3% uncertainty in the loss tangent results were caused mostly by the nonuniformity of the samples. The 5% error at 100 MHz resulted for similar reasons and in addition for the limited accuracy of the instrument itself.

Table 2
The sintered densities, cell parameter and average grain size of all specimens

Composition	Density (g/cm^3)	Cell parameters (A)	Average grain size (μm)
$Ba_{0.6}Sr_{0.4}TiO_3$	5.43	3.9639	5–12
$Ba_{0.6}Sr_{0.4}Mn_{0.01}Ti_{0.99}O_3$	5.35	3.949	4–7
$(Ba_{0.6}Sr_{0.4})_{0.99}Y_{0.01}TiO_3$	5.37	3.9451	0.5–1
$Ba_{0.6}Sr_{0.4}Co_{0.01}Ti_{0.99}O_3$	5.31	3.9626	5–8

Fig. 4 shows the applied dc field dependence of relative dielectric constant for all specimens at temperature 15 °C at 10 kHz. For the limit of the instrument, we cannot get tunability data at high frequency. Because there is not an absolute numerical correspondence between the low frequency and microwave frequency, so the low frequency tunability data are useful only as tunability trend indicator [9]. From the figure, it shows that the relative dielectric constant of all specimens decreases with increasing applied dc field. That the relative dielectric constant nonlinearly decreases with increasing applied dc field at the paraelectric state can be explained by the phenomenological theory Devonshire [10,11]. Based on the framework, Johnson proposed an expression for the dielectric constant under the dc field as:

$$\text{Tunability} = \frac{\varepsilon_{r(0)} - \varepsilon_{r(app)}}{\varepsilon_{r(0)}} \times 100\%, \quad (1)$$

$$\frac{\varepsilon_{r(app)}}{\varepsilon_{r(0)}} = \frac{1}{[1 + \alpha\varepsilon_{r(0)}^3 E^2]^{1/3}} \quad (2)$$

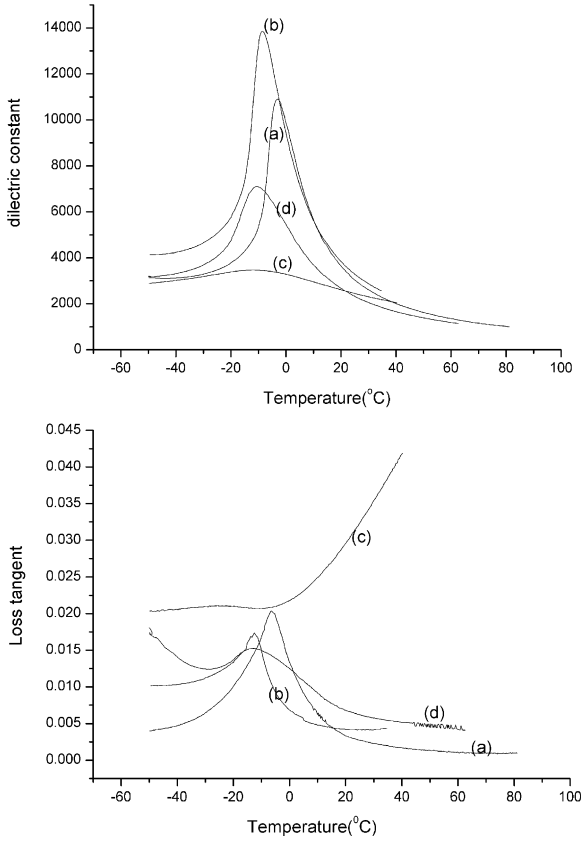

Fig. 3. Temperature dependence of the dielectric constant and loss tangent measured at 10 kHz: (a) $Ba_{0.6}Sr_{0.4}TiO_3$; (b) $Ba_{0.6}Sr_{0.4}Mn_{0.01}Ti_{0.99}O_3$; (c) $(Ba_{0.6}Sr_{0.4})_{0.99}Y_{0.01}TiO_3$; (d) $Ba_{0.6}Sr_{0.4}Co_{0.01}Ti_{0.99}O_3$.

where $\varepsilon_{r(0)}$ and $\varepsilon_{r(app)}$ are the dielectric constants under zero dc field and under the applied field, respectively, and α is the anharmonic coefficient. From the Eq. (2), we can see generally the higher the dielectric constant, the higher tunability. The anharmonic coefficient is assumed to be an order parameter of the anharmonic interactions. For the perovskite structure materials, the dc field effect at the paraelectric state is due to the anharmonic interactions of Ti^{4+} ions. To make Eq. (2) more simple, we get Eq. (3):

$$y = bx \tag{3}$$

where $y = (\varepsilon_0/\varepsilon')^3 - 1$, $x = E^2$, $b = a\varepsilon_0^3$ and from the definition of the tunability and we can see the tunability has the same trend with the coefficient b.

Based on Eq. (3), Fig. 5 presents a linearized plot of the experimental data of the doping $Ba_{0.6}Sr_{0.4}TiO_3$. The strait

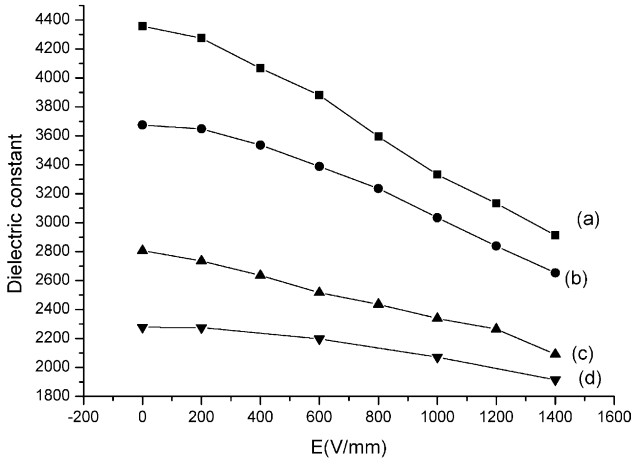

Fig. 4. dc field dependence of the dielectric constant for all the specimens at temperature 15 °C at 10 kHz: (■) $Ba_{0.6}Sr_{0.4}TiO_3$; (●) $Ba_{0.6}Sr_{0.4}Mn_{0.01}Ti_{0.99}O_3$; (▲) $(Ba_{0.6}Sr_{0.4})_{0.99}Y_{0.01}TiO_3$; (▼) $Ba_{0.6}Sr_{0.4}Co_{0.01}Ti_{0.99}O_3$.

lines and parameters shown in the figure were obtained by linear regressions; y and x represent the ordinate and abscissa as defined by the axes labels. The figure shows the experimental data can be linearized. But the route is not through the origin which is expected by Eq. (3) and this deviation from Eq. (3) may be attributed to the nonuniform dielectric constant of the specimens and instrumental errors [12]. So, the phenomenological equation proposed by Johnson can fit the experimental data well at paraelectric

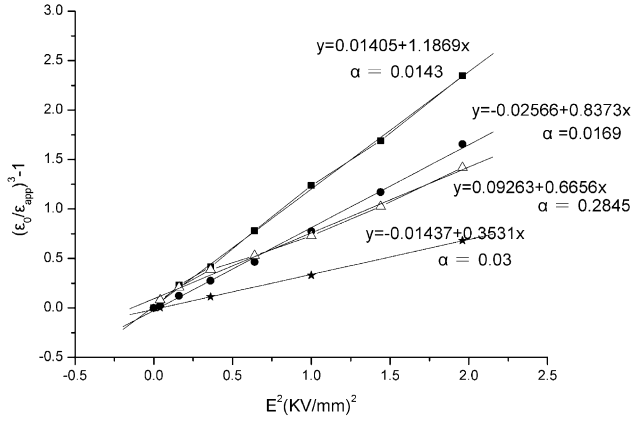

Fig. 5. Linearized plot of the electric-field dependence of the dielectric constant of the doping $Ba_{0.6}Sr_{0.4}TiO_3$. (■) $Ba_{0.6}Sr_{0.4}TiO_3$; (●) $Ba_{0.6}Sr_{0.4}Mn_{0.01}Ti_{0.99}O_3$; (Δ) $(Ba_{0.6}Sr_{0.4})_{0.99}Y_{0.01}TiO_3$; (★) $Ba_{0.6}Sr_{0.4}Co_{0.01}Ti_{0.99}O_3$. The straight lines are the linear fitting, the dot are the experimental data.

Table 3
The summary of measurements of different compositions at temperature 15 °C

Composition	Curie temperature (°C)	Loss tangent	
		10 kHz	100 MHz
$Ba_{0.6}Sr_{0.4}TiO_3$	−2.0 to −3.0	0.0046 ± 0.0001	0.023 ± 0.001
$Ba_{0.6}Sr_{0.4}Mn_{0.01}Ti_{0.99}O_3$	−8.5 to −9.0	0.0057 ± 0.0002	0.019 ± 0.001
$(Ba_{0.6}Sr_{0.4})_{0.99}Y_{0.01}TiO_3$	−12.0 to −13.0	0.026 ± 0.008	0.021 ± 0.001
$Ba_{0.6}Sr_{0.4}Co_{0.01}Ti_{0.99}O_3$	−10.0 to −11.0	0.0088 ± 0.0003	0.020 ± 0.001

Table 4
The summary of measurements of electric field dependence of dielectric behaviors for all specimens at temperature 15 °C

Composition	α ($\times 10^{-21}$) (m/v)^2	Tunability (%)[a]
$Ba_{0.6}Sr_{0.4}TiO_3$	0.0143	$T = (23.68 \pm 0.50)E$
$Ba_{0.6}Sr_{0.4}Mn_{0.01}Ti_{0.99}O_3$	0.0169	$T = (20.00 \pm 0.40)E$
$(Ba_{0.6}Sr_{0.4})_{0.99}Y_{0.01}TiO_3$	0.0285	$T = (18.20 \pm 0.35)E$
$Ba_{0.6}Sr_{0.4}Co_{0.01}Ti_{0.99}O_3$	0.03	$T = (16.40 \pm 0.30)E$

[a] T: tunability in %, E: electric field in kV/mm.

state of the doping $Ba_{0.6}Sr_{0.4}TiO_3$. From the figure, the parameter α of all the doping $Ba_{0.6}Sr_{0.4}TiO_3$ is higher than the undoped. This may be attributed to the addition of these dopant, which makes the unit cell smaller as shown in Table 2, resulting in a short distance between the Ti^{4+} ions. The vibration amplitude of center ions is softened much more easily by its nearest neighbours. This enhances the anharmonic effect and thus α increases [13]. The figure also indicates that the slope of the line b decreases when adding these dopants. As said before, b has the same trend with the tunability, so the tunability of the doping $Ba_{0.6}Sr_{0.4}TiO_3$ is lower than the undoped and this can be seen clear in Table 4.

4. Conclusions

The acceptor (Mn-, Co-) doping and donor Y-doping $Ba_{0.6}Sr_{0.4}TiO_3$ have been characterized. The results demonstrated that all the dopants have a strong effect on the grain size and the dielectric properties. The Curie temperature of the doping samples decreases. All the doped specimens increase loss tangent at temperature 15 °C at low frequency and at high frequency (100 MHz) all the specimens have similar loss tangent to the undoped. The tunability decreases when adding the acceptor or donor dopants and dc field dependence of the dielectric constant of all the doping specimens fits the Johnson's phenomenological equation well.

Acknowledgement

This work was financially supported by the National Defence Science and Technology Innovation Foundation of Chinese Academy of Sciences.

References

[1] V.K. Varadan, K.A. Jose, V.V. Varadan, R. Hughes, A novel microwave planar phase shifter, Microwave J. (1995) 244–255.
[2] F. De Flaviis, Planar microwave integrated phase-shifter design with high purity ferroelectric material, IEEE Trans. Microwave Theory Tech. 45 (1997) 963–969.
[3] R.W. Babbitt, T.E. Koscica, Planar microwave electric–optic phase shifters, Microwave J. (1992) 63–79.
[4] S.B. Herner, F.A. Selmi, V.V. Varadan, V.K. Varadan, The effect of various dopants on the dielectric properties of barium strontium titanate, Mater. Lett. 15 (1993) 317–324.
[5] J.W. Liou, B.S. Chiou, Dielectric characteristics of doped $Ba_{1-x}Sr_xTiO_3$ at the paraelectric state, Mater. Chem. Phys. 51 (1997) 59–63.
[6] S. Garcia, R. Font, J. Portelles, R.J. Quninones, J. Heiras, J.M. Siqueiros, Effect of Nb doping on (Sr, Ba)TiO_3 (BST) ceramics samples, J. Electroceram. 6 (2001) 101–107.
[7] N.H. Chan, D.M. Smyth, Defect chemistry of donor-doped $BaTiO_3$, J. Am. Ceram. Soc. 67 (1984) 285–288.
[8] M.W. Cole, P.C. Joshi, M.H. Ervin, M.C. Wood, R.L. Preffer, The influence of Mg doping on the materials properties of $Ba_{1-x}Sr_xTiO_3$ thin films for tunable device application, Thin Solid Films 374 (2000) 34–41.
[9] M.W. Cole, C. Hubbard, E. Ngo, M. Ervin, M. Wood, Structure–property relationship in pure and acceptor-doped $Ba_{1-x}Sr_xTiO_3$ thin films for tunable microwave device applications, J. Appl. Phys. 92 (2002) 475–483.
[10] K.M. Johnson, Variation of dielectric constant with voltage in ferroelectrics and its application to parametric devices, J. Appl. Phys. 33 (1962) 2826–2831.
[11] H. Diamond, Variation of permittivity with electric field in perovskite-like ferroelectrics, J. Appl. Phys. 32 (1961) 909–915.
[12] A. Outzourhit, J.U. Trefny, Tunability of the dielectric constant of $Ba_{0.1}Sr_{0.9}TiO_3$ ceramics in the paraelectric state, J. Mater. Res. 10 (6) (1995) 1411–1417.
[13] S.G. Lee, D.S. Kang, Dielectric properties of ZrO_2-doped (Ba, Sr, Ca)TiO_3 ceramics for tunable microwave device applications, Mater. Lett. 57 (2003) 1629–1634.